Driving Towards Energy Efficiency: A Novel Torque Allocation Strategy for In-Wheel Electric Vehicles

Fadel Tarhini, Reine Talj, Moustapha Doumiati

Driving Towards Energy Efficiency: A Novel Torque Allocation Strategy for In-Wheel Electric Vehicles

Fadel Tarhini[1], Reine Talj[1] and Moustapha Doumiati[2]

***Abstract*— Electric vehicles (EVs) with four independent in-wheel motors are classified as over-actuated systems, granting unprecedented possibilities to meet the total driving torque and yaw moment demands through an infinite number of feasible torque combinations. Ensuring an energy-efficient torque distribution among the motors is indispensable for mitigating energy consumption and extending the driving range. This is a pivotal factor in promoting eco-friendly and sustainable transportation solutions. This work focuses on the low-level control of a proposed multi-objective control architecture, encompassing longitudinal, lateral, stability, and maneuverability control. A novel configuration method for torque allocation is established, followed by developing and contrasting four multi-objective-based strategies. An energy-saving criterion is further developed, and the energy-efficient allocation strategies are carried out within the frameworks of online and offline optimization, based on the Sequential Quadratic Programming (SQP) algorithm. The proposed architecture is tested and validated in a joint simulation between Simulink/MatLab and SCANeR^{TM} Studio vehicle dynamics simulator. The simulation outcomes demonstrate that implementing the suggested torque allocation can lead to enhancements in the energy efficiency, driving comfort, and stability of the electric vehicle.**

I. Introduction

The adoption of electric power as a means of transportation is increasingly gaining momentum in mitigating the adverse effects of traditional combustion engines and fossil fuels on the environment. Electric vehicles have devoted considerable attention to many due to their efficient energy use, emission-free operation, and exceptional driving capabilities. On the other hand, statistical data show that 90% of accidents occur as a result of driver incompetence [1]. Hence, research studies are moving towards Autonomous Vehicles (AVs) to improve road safety.

Electric vehicles equipped with four in-wheel motors have attracted enormous attention in the literature and industry because of their actuation flexibility [2] and potential for reducing energy consumption [3]. These vehicles benefit from an over-actuated system that allows for independent control of each actuator, serving both traction and braking purposes. As a result, leveraging the unique features of such systems opens up possibilities for designing advanced controllers that can enhance vehicle performance while simultaneously reducing energy consumption.

The development of autonomous vehicles is rapidly advancing, and the focus is shifting toward optimizing their energy efficiency by integrating in-wheel motors. One widely applied and effective method to control such systems is torque allocation. This method involves regulating the vehicle's motion by allocating torques on the wheels using independent in-wheel motors and solving constrained control allocation problems to minimize various cost functions. The cost function may prioritize safety [4], energy consumption [5], or multi-objective criteria [6]. Thus, it is a concise and modular approach to optimizing dynamic trade-offs between vehicle performance and energy efficiency.

To effectively distribute torques among the four independent in-wheel motors, Control Allocation (CA) strategies often leverage optimization algorithms. Notably, there are several approaches that target energy-efficient control. For instance, the energy-efficient control in [7] is classified as a minimization of both the tire friction loss and the power consumption of the electric motor. An energy optimal trajectory tracking control for an autonomous in-wheel driven vehicle considering maximizing battery State Of Charge is done in [8]. A hybrid model predictive control is implemented by [9] to minimize the drive-train power loss while ensuring vehicle stability. Particle Swarm Optimization (PSO) is employed in [10] to solve a real-time optimal distribution strategy with the aim of maximizing the motors' utilization in high-efficiency zones. [11] proposed an energy-efficient and real-time implementable torque allocation strategy based on minimizing power losses using offline optimization. An Energy Efficient Cruise Control is developed in [12] to operate the EV's power train close to its peak efficiency region. Other strategies considered different objectives. For instance, [13] presented a control allocation strategy to optimize the tire forces of a hybrid EV. Whilst, an integrated control strategy is developed in [14] to improve energy economy and longitudinal driving stability. However, traction torques are distributed to handle stability on low-adhesion roads independently of energy economy which is promoted on high-adhesion roads.

Literature shows that the control of the vehicle performance is often treated independently of the energy aspects, whereas electric AVs have a significant potential for reducing energy consumption. In this paper, a multi-objective control architecture is developed. As the work considers a fully autonomous vehicle, lateral control conjugated with longitudinal control is established at the high level, in addition to the stability and maneuverability control objectives [15]. The paper focuses on the low level where the desired objectives are achieved by physical actuators, including the four In-wheel Motors and the Active Front Steering (AFS). The high-level control inputs are assumed to be generated at each time step and sent to a torque allocation unit, where a novel torque allocation method is proposed to distribute the traction and braking torques among the motors. An energy consumption optimization criterion is illustrated based on a developed consumption model. Then, four multi-objective strategies are developed and contrasted to examine the energy consumed by each one. Each strategy presents an optimal allocation considering its corresponding objectives, where the online and offline strategies are executed using the SQP method based on an utter energy economy objective.

[1]Sorbonne université, Université de Technologie de Compiègne, CNRS, Heudiasyc UMR 7253, CS 60 319, 60 203 Compiègne, France.

[2]ESEO-IREENA lab UR 4642, Nantes Université, 10 Bd Jeanneteau, 49100 Angers, France.

The paper contributions are stated as:

- Establishment of a novel approach for torque allocation, by imposing the constraints on the low level control.
- Development of an energy consumption model, with a criterion to determine the saved energy based on a constructed performance index.
- Development and comparison of four strategies for optimal torque distribution considering multi-objectives.

The paper is structured as follows: Section II illustrates the multi-objective control architecture, by exposing the high level and introducing the allocation strategy at the low level. Section III presents the energy-saving criterion based on a proposed energy performance index. The four multi-objective-based strategies are revealed in Section IV. Finally, a discussion of the results is presented in Section V, followed by a conclusion.

II. Multi-Layer Control Architecture

A. Decentralized Control Architecture

The complete developed control architecture is given in Fig. 1. Aside from the perception and localization part, it consists of three layers: decision and control at the high level, and actuators coordination at the low level. The architecture is structured based on a decentralized control [16], where control commands representing the desired objectives are generated. The objectives originated in this study are lateral and longitudinal control, as well as maneuverability and stability control. Lateral control is achieved by regulating the steering angle δ_c of the Active Front Steering (AFS) actuator. Longitudinal control is executed by controlling the longitudinal velocity V_x of the vehicle, by distributing a generated total driving torque T_m among the four in-wheel motors. Lastly, stability and maneuverability are switched according to the driving situation. A risk of instability is detected by a decision-layered stability monitor, directly promoting the stability objective while relaxing maneuverability. Stability is restored by controlling the side-slip angle β, while maneuverability control is attained by controlling the yaw rate $\dot{\psi}$ of the vehicle. The latter objectives are realized by generating a corrective yaw moment M_z using the Direct Yaw Control (DYC). The generated driving torque and the yaw moment are received by a torque allocation unit to generate four driving and four braking torques among the motors. Finally, the controlled steering and the generated torques are fed into the fully dynamic "Callas" vehicle of the SCANeR^{TM} Studio simulator.

B. High Level Control

The high level is composed of three decentralized controllers based on the Super Twisting Sliding Mode Control (STSMC), which generates control inputs in order to control independently, the vehicle's lateral and longitudinal dynamics, as well as its stability and maneuverability. This work builds upon our previous publication on high-level control [15], so it will not be elaborated on in this paper. The reader can refer to [17] for method implementation.

C. Low Level Control

Following the generation of the control inputs for lateral, longitudinal, stability/maneuverability control objectives at the high level, δ_c is realized by AFS at the low level. M_z is achieved using the DYC by distributing the torques among

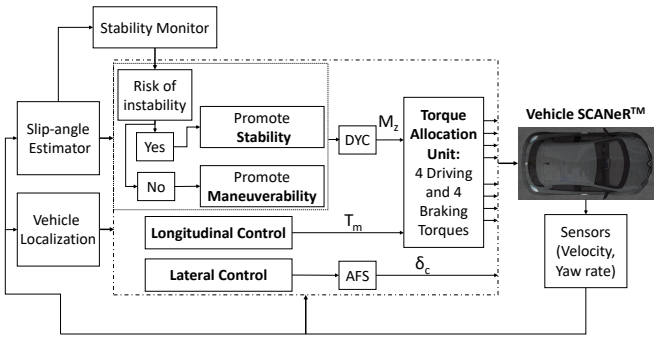

Fig. 1: Schematic diagram of the proposed architecture

the motors, along with T_m within a torque allocation unit. To benefit from the advantages of the system's over-actuation, torques must be dispersed using the maximum possible degrees of freedom (DOF). Indeed, there are 4 driving and 4 braking torques that can be realized by the actuators, however, there is a set of constraints to be imposed on the distribution configuration, hence decreasing the number of possible DOF. To avoid interference with the generation of M_z, every wheel on the same axle must receive similar torques, and the sum of the four driving torques must be equal to T_m (1).

$$\begin{aligned} T_m &= T_{d,rl} + T_{d,rr} + T_{d,fr} + T_{d,fl} \\ T_{d,il} &= T_{d,ir} \end{aligned} \tag{1}$$

where $T_{d,ij}$ is the driving torque acting on the wheel ij, and i, j = [rear (r), front (f)], [right (r), left (l)]. Imposing these constraints on $T_{d,ij}$, the driving torques allocation (2) resulted. Therefore, the total motor torque T_m is weighted by a variable p on the front axle, and $(1-p)$ on the rear one.

$$\begin{cases} T_{rl} = T_{rr} = \frac{T_m}{2}(1-p) \\ T_{fl} = T_{fr} = \frac{T_m}{2}(p) \end{cases} \quad \text{where } 0 \leq p \leq 1 \tag{2}$$

The constraints (1) are imposed into the variable p and modulated as p between 0 and 1. To enable the development of M_z utilizing the four wheels, its generation is split between the vehicle's front and rear sides, resulting in two centers of rotation, one on each of the front and rear axles. This is done by weighting M_z by a parameter k on the rear axle and $(1-k)$ on the front one. The moment is converted into wheel torque by multiplying it by the ratio of the wheel effective radius r over the half track t_r. Therefore, M_z is formed by generating two total torques T_r and T_f on the rear and front axles respectively.

$$\begin{cases} T_r = \frac{-r}{t_r}\, kM_z \\ T_f = \frac{-r}{t_r}\, (1-k)M_z \end{cases} \quad \text{where } 0 \leq k \leq 1 \tag{3}$$

Assuming small δ and considering a counter-clockwise (ccw) M_z generation,

$$\frac{M_z}{t_r} = -F_{x,rl} + F_{x,rr} - F_{x,fl} + F_{x,fl} \tag{4}$$

where $F_{x,ij}$ is the wheel ij longitudinal force. T_r and T_f are distributed between the left and right sides by a combination of deceleration and acceleration on the vehicle's both sides according to the direction of M_z. In order to avoid excessive

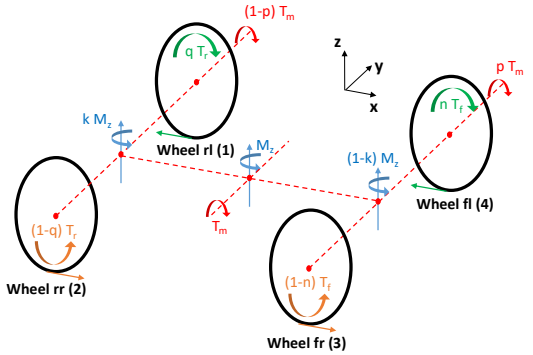

Fig. 2: Proposed torque allocation for a ccw M_z

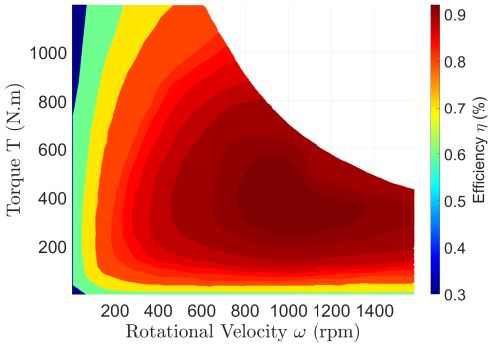

Fig. 3: In-wheel motor efficiency: motoring (η_d)

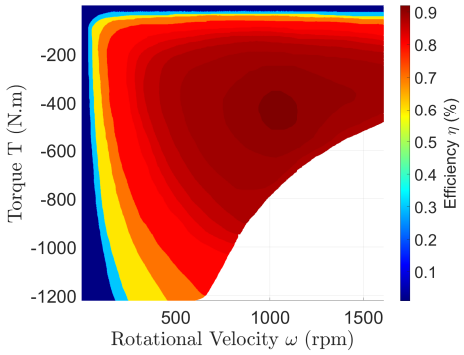

Fig. 4: In-wheel motor efficiency: regenerative braking

acceleration/braking, T_r and T_f are distributed such that wheels on the same side receive the same sense of torque (acceleration or braking), and the wheels on the same axle receive opposite torque senses. These constraints, along with (4) are imposed in the parameters k, q, n. The distribution between both sides of the vehicle is done by weighting the total rear torque T_r by q for braking and $(1-q)$ for accelerating. Similarly, T_f is weighted by n for decelerating and $(1-n)$ for accelerating.

$$\begin{cases} T_{b,rr} = qT_r \\ T_{b,fr} = nT_f \\ T_{d,rl} = (1-q)T_r \\ T_{d,fl} = (1-n)T_f \end{cases} \quad \text{where} \quad q, n \in [0, \ \ 1] \tag{5}$$

The distribution depends on the direction of M_z. If the required M_z is in cw direction, torques are distributed as in (5). Otherwise, distribution is done according to (6).

$$\begin{cases} T_{b,rl} = qT_r \\ T_{b,fl} = nT_f \\ T_{d,rr} = (1-q)T_r \\ T_{d,fr} = (1-n)T_f \end{cases} \quad \text{where} \quad q, n \in [0, \ \ 1] \tag{6}$$

where $T_{b,ij}$ represent the wheel ij braking torque. Combining (2, 3, 5, 6) leads to the allocation (7) for ccw M_z and (8) otherwise, where $p, k, q, n \in [0, \ 1]$.

$$\begin{cases} T_{b,rl} = q\frac{-r}{t_r}\, kM_z \\ T_{b,fl} = n\frac{-r}{t_r}\, (1-k)M_z \\ T_{b,rr} = Tb_{fr} = 0 \\ T_{d,rl} = (1-p)\frac{T_m}{2} \\ T_{d,rr} = (1-p)\frac{T_m}{2} + (1-q)\frac{-r}{t_r}\, kM_z \\ T_{d,fl} = p\frac{T_m}{2} \\ T_{d,fr} = p\frac{T_m}{2} + (1-n)\frac{-r}{t_r}\, (1-k)M_z \end{cases} \tag{7}$$

$$\begin{cases} T_{b,rr} = q\frac{r}{t_r}\, kM_z \\ T_{b,fr} = n\frac{r}{t_r}\, (1-k)M_z \\ T_{b,rl} = Tb_{fl} = 0 \\ T_{d,rr} = (1-p)\frac{T_m}{2} \\ T_{d,rl} = (1-p)\frac{T_m}{2} + (1-q)\frac{r}{t_r}\, kM_z \\ T_{d,fr} = p\frac{T_m}{2} \\ T_{d,fl} = p\frac{T_m}{2} + (1-n)\frac{r}{t_r}\, (1-k)M_z \end{cases} \tag{8}$$

Therefore, the traction and braking torques are distributed according to the illustrated configuration Fig 2, depending on four parameters p, k, q, n. Imposing the constraints on the low level to be directly carried by the four parameters reduces the computational time of the allocation, simplifies the problem formulation, and clarifies the feasibility of the optimization problem defined later.

III. Energy Consumption Model

A. Power Consumption

The power consumption of the four motors can be defined as (9) in dependence on the efficiency of each motor. As the power loss of the battery is considered negligible, the output power of the battery P_{bo} equates to the total power consumption of the motors. Thus:

$$P_{bo} = \sum_{i=1}^{4} P_i = \sum_{i=1}^{4} \frac{T_i \omega_i}{\eta_{k,i}^{sign(T_i)}} \tag{9}$$

where $\eta_k = \eta_d$ corresponding to motoring/driving efficiency if $T_i \geq 0$, whilst $\eta_k = \eta_b$ corresponding to regenerative braking efficiency otherwise. The motor efficiency depends on the torque generated by the motor and its angular velocity. The relation $\eta = f(T, \omega)$ is denoted by the motor efficiency MAP. Due to the high order and nonlinearity of the motor system, obtaining an explicit form of efficiency is extremely difficult. Thus, the efficiency estimation is performed using Look-Up Tables (LUTs) visualized in the form of MAPs. The efficiency MAPs for the PD18 DC electric in-wheel motor [18] are constructed for motoring (traction torques) and for regenerative braking (braking torques) in Figures 3, 4 respectively. Finally, the efficiency η is estimated through the LUT based on a linear point-slope interpolation using the binary search method.

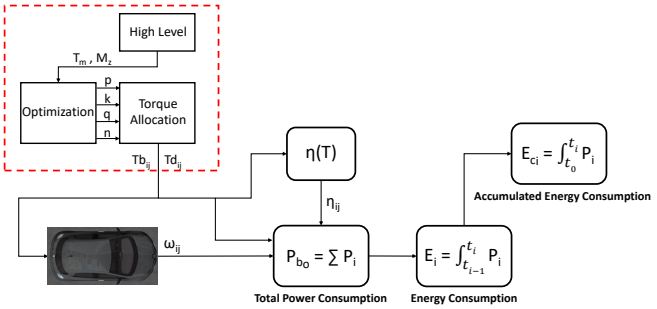

Fig. 5: Consumption model illustration

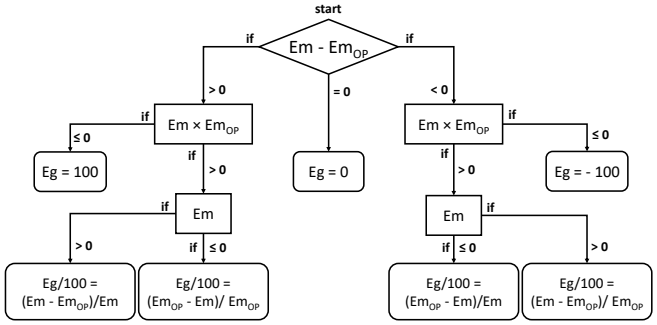

Fig. 6: Proposed energy performance index E_g (%)

B. Accumulated Energy Consumption

The process of accumulation of energy consumption is a way to determine the amount of energy consumed by the battery in a sustained manner. It is the entire consumed energy from the initial instant t_0 until the current instant t_i. It can be determined by accumulating the pre-consumed energies at each interval (Fig. 5).

C. Percentage Energy Gain

The criterion to determine the amount of energy saved as a result of the optimization is to compute the relative change in energy consumption from a vehicle with optimized torque distribution to a vehicle without. The comparison is performed with a reference vehicle (denoted by "classical vehicle"), which is distinguished by distributing the traction torques uniformly on the four wheels and generating M_z using half-traction/ half-braking on the vehicle's opposite sides. Adapted to the proposed strategy, the classical vehicle torque distribution is: $p = k = q = n = 0.5$. Therefore, the criterion is to apply the performance energy index E_g (see Fig. 6) on the accumulated energy consumption of the two vehicles, where $E_{m_{OP}}$ and E_m are respectively, the energy consumed by the vehicle with optimized torque distribution and the classical vehicle.

Energy gain E_g depicts the percentage of energy saved by virtue of distributing the torques optimally, considering minimizing the energy consumption. The total energy gain represents the overall saving percentage, specified by the final instant t_f at the end of the test.

D. Energy Consumption Optimization

The high-level constraint that torque allocation is dependent on control inputs generated at the current time instant limits power consumption to be instantaneous and drives its realization to be unanticipated.

$$E_{tot} = \int P_{bo}\, dt = \int \sum_{i=1}^{4} \frac{T_i \omega_i}{\eta_{k,i}^{sign(T_i)}}\, dt \tag{10}$$

The objective function desired to be minimized is the total energy given in (10). Since the power consumption can't be predicted, the integration of the battery power couldn't be formalized. Hence, instead of minimizing the energy consumption over a time zone, it is sufficient to minimize the instantaneous power consumption. Therefore, the minimization of E_{tot} is equivalent to minimizing P_{bo} per sample time (11). This concept is held when the power loss of the battery is neglected [19].

$$min \int P_{bo}\, dt \Leftrightarrow min\, P_{bo} \tag{11}$$

Hence, the problem is transformed into an instantaneous optimization problem of determining T_i satisfying (12), i.e. the optimization problem turns into finding the four parameters p, k, q, n at each instant, that minimizes a cost function which resembles the power consumption.

$$\min_{T_i(p,k,q,n)} \quad \sum_{i=1}^{4} \frac{T_i \omega_i}{\eta_{k,i}^{sign(T_i)}} \tag{12}$$

IV. Multi-Objective-Based Strategies

The reduction of the vehicle's energy consumption entails finding the optimal parameters' values that minimize a cost function that reflects the desired objectives. Any set of values for p, k, q, n that satisfies their constraints $[0, 1]$ represents a feasible solution for the optimization problem (12). Four strategies are developed considering multi objectives, where the energy consumption is studied in each case.

A. Constant Parameters: "Constant Strategy"

The term "constant parameters" refers to the practice of keeping the allocation parameters p, k, q, and n at fixed, unchanging values. This term is derived from the idea of setting these parameters as constants:

$$p = \frac{l_r}{l_f + l_r}; \quad k = \frac{l_f}{l_f + l_r}; \tag{13a}$$

$$q = \frac{t_r}{t_f + t_r}; \quad n = \frac{t_f}{t_f + t_r}, \tag{13b}$$

where l_r and l_f are the distances from the center of gravity to the rear and front axles respectively, and t_r and t_f are the half-rear and half-front tracks respectively. In this paper, the tested vehicle has similar tracks ($t_r = t_f$) which in terms effectuate assigning q, n as $1/2$, forcing the sum of the longitudinal forces acting on the wheels to become 0. This minimizes interference with the longitudinal dynamics.

B. Dynamic Load Distribution: "Dynamic Strategy"

The Tire Working-Load Usage (TWU) (14) as defined in [20] represents the edges of the friction circle. The basic idea behind the friction circle is to impose a limit on the longitudinal forces $F_{x,i}$ acting on the wheels due to the existence of the lateral forces $F_{y,i}$. As TWU is smaller i.e. the friction circle of the wheel is larger, as the wheel has

more adhesion to the ground, thus has the ability to have larger torques.

$$TWU = \sum_{i=1}^{4} \frac{F_{x,i}^2 + F_{y,i}^2}{(\mu F_{z,i})^2} \tag{14}$$

The load distribution ratio κ is defined as

$$\kappa = \frac{F_{z,f}}{F_{z,r}} = \frac{F_{z,fr} + F_{z,fl}}{F_{z,rr} + F_{z,rl}} \tag{15}$$

The strategy is to make the ratio of the longitudinal forces proportional to the loads Fz_i, between the rear and front sides of the vehicle. Hence, κ is reformulated as

$$\kappa = \frac{F_{x,f}}{F_{x,r}} = \frac{pT_m/r}{(1-p)T_m/r} \tag{16}$$

Therefore, the allocation parameters are formulated as

$$\begin{aligned} p &= \frac{F_{z,f}}{F_{z,f} + F_{z,r}} = \frac{\kappa}{1+\kappa} \\ k &= 1 - p = \frac{1}{1+\kappa} \\ q &= n = \frac{1}{2} \end{aligned} \tag{17}$$

where q and n are assigned as 0.5 to preserve the longitudinal dynamics. Note that for an on-road vehicle, the tire normal forces can be estimated in real-time by implementing an Extended Kalman Filter observer (see [21]).

C. Online Optimization: "Online Strategy"

Numerical optimization is a process that involves generating a sequence of estimates of the solution, culminating either in arriving at the solution or coming sufficiently close. Solving this problem requires a set of tools or methods including the SQP algorithm. The SQP method can be viewed as a generalization of Newton's method for unconstrained optimization in that it finds a step away from the current point by minimizing a quadratic model of the problem. The general form of a nonlinearly constrained optimization problem is given in (18).

$$\min_{x \in \mathcal{R}^n} f(x) \quad \text{subject to} \begin{cases} c_i(x) = 0 & \forall\, i \in \mathcal{E} \\ c_i(x) \geq 0 & \forall\, i \in \mathcal{I} \end{cases} \tag{18}$$

where f and c_i are smooth scalar functions over $A \subset \mathcal{R}^n$, $\mathcal{E}$ denotes the set of equality constraints and $\mathcal{I}$ the set of inequality constraints. The SQP algorithm replaces the objective function with the quadratic approximation (19), and replaces the constraint functions with linear approximations.

$$q_k(d) = \nabla f(x_k)^T d + \frac{1}{2} d^T \nabla^2_{xx} \mathscr{L}(x_k, \lambda_k) d \tag{19}$$

where the step d is calculated by solving the quadratic subprogram (20) (which is easier to solve and its objective function can reflect the nonlinearities of the original problem).

$$\begin{aligned} \min \{ q_k(d) \ :\ & c_i(x_k) + \nabla c_i(x_k)^T d \leq 0,\ i \in \mathcal{I}; \\ & c_i(x_k) + \nabla c_i(x_k)^T d = 0,\ i \in \mathcal{E} \} \end{aligned} \tag{20}$$

The computation of $\nabla^2_{xx} \mathscr{L}(x_k, \lambda_k)$ is replaced by the BFGS (Broyden-Fletcher-Goldfarb-Shanno) approximation B_k, which is updated at each iteration [22]. The local convergence of the SQP approach is satisfied when (x^*, λ^*) satisfies the second-order sufficiency conditions. If the starting point x_0 is sufficiently close to x^*, and the Lagrange multiplier estimates λ_k remain sufficiently close to λ^*, then the sequence generated by setting $x_{k+1} = x_k + d$ (k is an iteration index) converges to x^* at a second-order rate. The implementation consists of consecutive stages of updating the Hessian matrix, Quadratic Programming solution, Initialization, and Line Search and Merit Function (see [23]).

The method is implemented by minimizing a cost function $f(x)$, representing a quantitative measure of the performance of the system under study. Since the constraints are already imposed at the low level and carried by the parameters p, k, q, and n, one can define the optimization problem as

$$\min_x f(x) \quad \text{subject to} \begin{cases} Ax \leq b \\ l_b \leq x \leq u_b \end{cases} \tag{21}$$

where $x = [p\ k\ q\ n]^T$, represents the vector of the optimization variables. $l_b = [0\,0\,0\,0]^T$ and $u_b = [1\,1\,1\,1]^T$ are the lower and upper bounds for x respectively. x_0 is initialized by assigning 0.5 to each variable as a midway between l_b and u_b. The cost function reflects the total power consumption of the motors (22). The acceleration torques depend on T_m and p, while the deceleration torques are a function of M_z and k, q, n. When reformulating, $f(x)$ is converted into an equation governed by the high-level generated control inputs, and function of the optimization parameters.

$$f(x) = \sum_{i=1}^{4} \frac{T_i(x)\ \omega_i}{\eta_{k,i}^{sign(T_m)}} \quad \text{where } x = [p, k, q, n] \tag{22}$$

A fast fluctuation between 0 and 1 is observed in p, translated by assigning the traction torques to the axle whose wheels have lower angular velocities. The oscillation exhibited no effect on the chassis, after the study of the behavior of κ, pitch and roll angles, and the load transfer ratio. However, the high-frequency signals are naturally filtered by the motor actuator. The rapid switching between the front and rear wheels won't be entirely realized. A simplified first-order electric model is applied (23), to study the effect of the natural filtering of the motor actuator as in [24].

$$T^*_{ij} = \frac{1}{1 + \frac{L_m}{R_m} s}\ T_{ij} \tag{23}$$

where L_m and R_m are respectively the motor's internal inductance and resistance, T_{ij} is the requested torque at the low level, and T^*_{ij} corresponds to the motor-generated torque. Parameters q and n carried a singular value 1, reflecting the generation of M_z through braking torques only. Its justification lies in the regenerative braking system (RBS), where the system favors activating DYC through braking, in order to gain energy instantaneously. However, by braking repeatedly, the chassis loses its inertia and will be forced to re-accelerate to compensate for the errors on V_x, consequently losing energy. To solve this problem, the online optimization problem is divided into two steps.

Proposed Two-Step Multi-Objective Algorithm:

In the first step, q, n parameters are assigned according to multi objectives, then p, k parameters are determined in the second step. The DYC controller is always active, either

Algorithm Two-Step Optimization

procedure GET-Q,N(M_z)
  if $|M_z| \leq \underline{M_z}$ **then**
    Activate DYC using traction torques only
  else if $\underline{M_z} < |M_z| \leq \overline{M_z}$ **then**
    Activate DYC $\frac{1}{2}$ traction/ $\frac{1}{2}$ braking torques
  else
    Activate DYC using braking torques only
  end if
end procedure
procedure GET-P,K($T(x)$, ω, η, q, n)
  $x = \arg\min_{x} \; f(T_{(x)},\ \omega,\ \eta_{\,(T,\,\omega)})$ ▷ x = [p, k]
end procedure

for maneuverability or stability. Hence, if M_z is always generated by braking, it will cause driving discomfort and wear on the wheels. Therefore, for low $|M_z|$ ($< \underline{M_z}$), reflecting normal driving, step 1 favors operating DYC by traction torques only. This helps avoid wear of the wheels, assists in a comfortable drive, and provides higher V_x. For mid $|M_z|$, imposing the vehicle in low error on the side-slip angle or high yaw rate error, step 1 favors the generation of M_z by half traction/braking. This will preserve the longitudinal dynamics, providing a counterbalance, earning some energy, and avoiding excessive acceleration/braking. Lastly, if $|M_z| > \overline{M_z}$, the vehicle is in a critical situation and exposed to high stability error. This often happens when facing a high cornering, or a sudden steering. To ensure safety, the vehicle must be slowed down and the traction torques must be averted. Hence, M_z is generated by braking torques only, consequently earning high energy. In the second step, p, k are determined by minimizing the cost function, considering the preassigned values for q, n.

D. Offline Optimization: "Offline Strategy"

An offline data-driven optimization is executed based on historical data and using the same methodology as in online optimization. Data (M_z, T_m, ω_i, etc..) are extracted prior to optimization by simulating the motion of the controlled vehicle. Then for each vehicle position, correspondent data are processed offline to determine the set of parameters p, k, q, n. Finally, re-input the optimized parameters corresponding to each position, under the same conditions. This offline method can be implemented with a Model Predictive Control (MPC) controller, in which the latter anticipates the vehicle situation in the near future, allowing to draw out some data. The offline processing of data, broke the time-dependency of the optimization parameters, meaning the instantaneous distribution won't affect the vehicles' parameters. In this way, therefore, the oscillation behavior of p, k will be averted.

V. Simulation Results

The proposed allocation strategy is implemented in the control architecture and tested in a co-simulation between Simulink/MatLab and SCANeR™ Studio vehicle dynamics simulator. In order to contrast the four proposed strategies, several simulations are conducted in the same testing environment. The accumulated energy consumption is marked in each strategy as it is the main cost variable in the comparison. Since the strategies are multi-objective-based, the corresponding advantages are highlighted in each case.

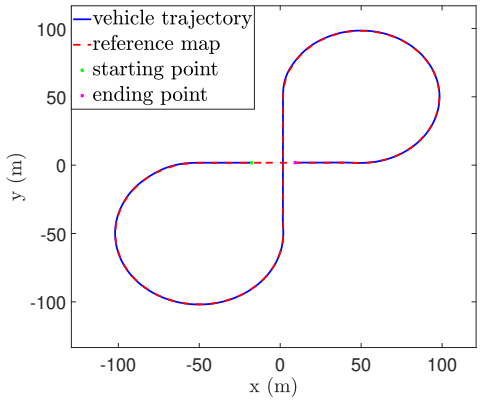

Fig. 7: Vehicle trajectory on the reference map

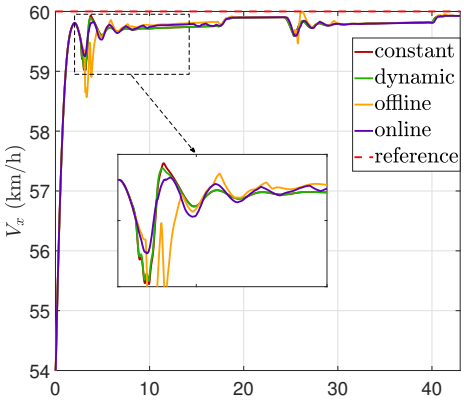

Fig. 8: Longitudinal velocities of the strategies

The autonomous vehicle is driven on the "infinity loop" track given in Fig. 7, representing a hard road geometry. The desired reference velocity is set 60 km/h, while the vehicle started the test at 54 km/h. The longitudinal velocity of each strategy is presented in Fig. 8. It can be observed that the velocities of the constant and dynamic strategies are the most conserved. The traction and braking torques of each motor corresponding to the constant strategy are shown in Fig. 9. The distribution of the torques in this strategy is performed based on a static load distribution by taking the wheelbase as a factor. Aside from the part of the traction torques dedicated to the yaw moment generation, the ratio of the torques between the front and rear axles is constant yet never 1. For the dynamic strategy, the torques are given in Fig. 10. The allocation is biased towards the front axle as the load distribution ratio κ varies around 1.5. As this strategy accounts for the dynamic transfer of the load between the rear and front axles, it is more robust to road-changing situations and more stable during high cornering. And since it considers a criterion for the minimization of the tire utilization rate, it is the most stable strategy against lateral skidding that results from tire saturation. The driving/braking torques of the online strategy are shown in Fig. 11. The exhibited oscillations arise due to the switching between the rear and front drive. This is a cost associated with using instantaneous optimization rather than optimizing over a time horizon. Observably, the implementation of the two-step optimization approach in the online strategy leads to a reduction in braking

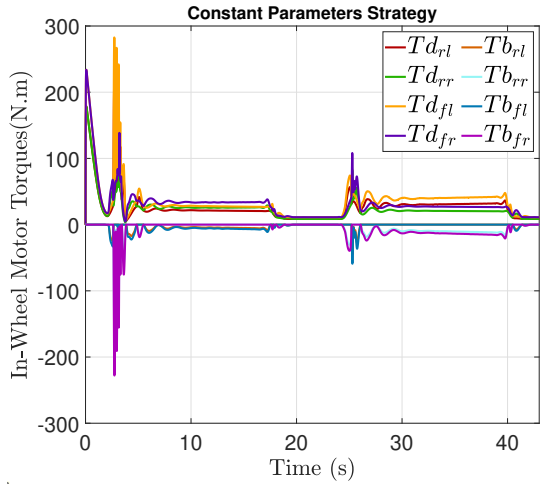

Fig. 9: In-wheel motor torques: constant strategy

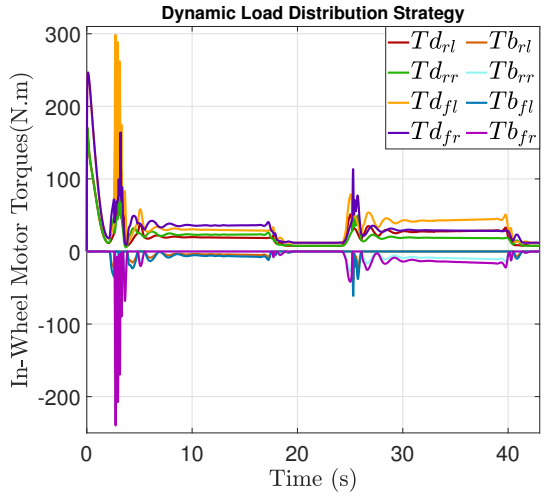

Fig. 10: In-wheel motor torques: dynamic strategy

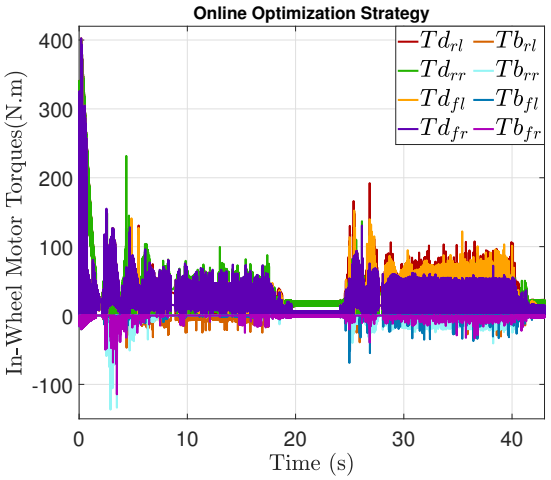

Fig. 11: In-wheel motor torques: online strategy

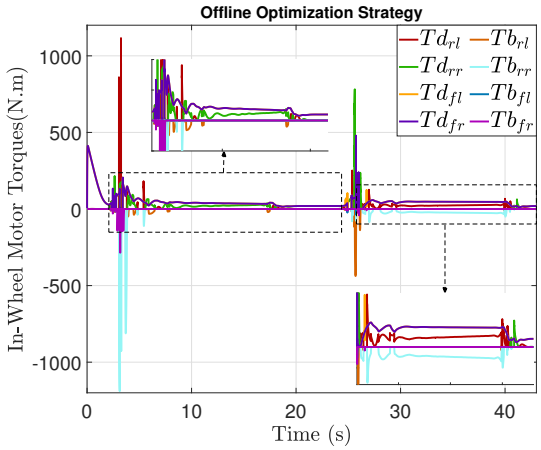

Fig. 12: In-wheel motor torques: offline strategy

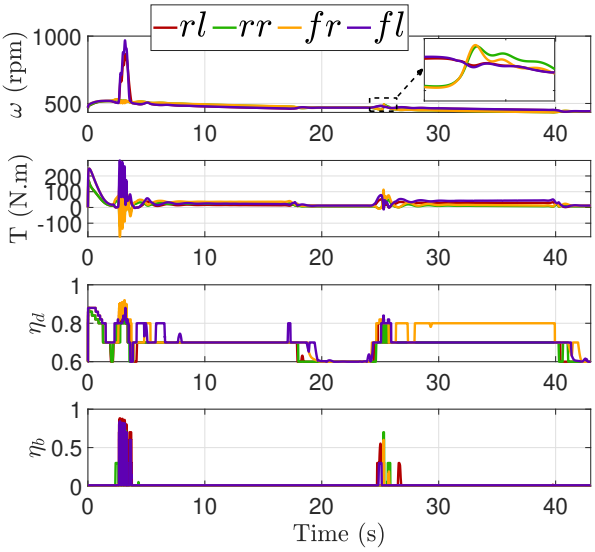

Fig. 13: In-wheel motor efficiency: dynamic strategy

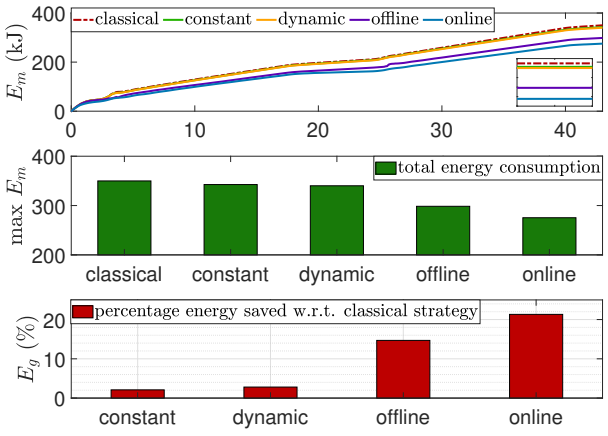

Fig. 14: Comparison of strategies: energy consumption

torques. The oscillations accompanying the optimization are prohibited in the offline strategy, where the torques are given in Fig. 12. The optimal allocation in this case results in an enhanced performance than the non-optimized case over a time horizon. Note that in order to fully use the advantages of the offline strategy, an MPC controller could be implemented where the optimization is executed on fixed predicted horizons and progressively updated. The estimation of the driving and regenerative braking efficiencies η_d and

η_b respectively is shown for the dynamic strategy only due to lack of space. Fig. 13 displays the variation of η_d and η_b as a function of motor rotational speed (ω) and its corresponding total traction/braking torque (T). When the demanded torque is traction, no regenerative braking is presented (η_b is minimum) and vice versa. Moreover, since the front axle motors generated torques higher than the rear axle motors, they have operated in higher efficiency zones.

The procedure of determining the amount of energy saved as a result of optimization entails calculating the total accumulated energy of the vehicle with optimal allocation and contrasting it with the classical strategy. Fig. 14 presents the accumulated energy consumption of all strategies. The classical strategy of uniformly utilizing the motors for traction and braking has marked the highest consumption. Followed by the constant, dynamic, offline, and the least energy consumption for online optimization. Finally, applying the energy performance index, and with respect to the classical strategy, the amount of energy saved in the constant strategy is $2.09\ \%$. As for the dynamic, offline, and online strategies are respectively $2.8\ \%$, $14.7\ \%$, and $21.3\ \%$. Although their objectives are independent of reducing energy, the constant and dynamic strategies have revealed an energy economy. This demonstrates that an optimal allocation considering a balanced load transfer (static or dynamic) is effective in preserving energy.

The configuration of the torque distribution plays an important role in the total performance of the vehicle. It has been demonstrated that the variation of the strategy to assign values for p, k, q, n, results in a diverse demeanor of the vehicle. This manifests the effectiveness of the proposed torque allocation strategy that encloses the problem into finding the parameters' values representing the optimal merits that correspond to the desired objectives.

VI. Conclusion

This paper presents the development of a multi-objective control architecture aimed at achieving lateral, longitudinal, stability, and maneuverability control. The study focuses on achieving these objectives through a novel torque allocation method at the low level, which distributes braking/traction torques through the four independent in-wheel motors. Further, an energy consumption model is developed based on constructed efficiency MAPs, introducing new notions that assist the criterion of determining the saved energy through a proposed energy index. Four multi-objective-based strategies are developed and compared with a classical strategy to differentiate vehicle performance and energy consumption reduction. As a future study, the proposed torque allocation strategy will be tested on real-world testing platforms.

ACKNOWLEDGMENT

This work is carried out within the framework of the V3EA project "Electric, Energy Efficient, and Autonomous Vehicle" (2021-2025), funded by the Research National Agency (ANR) of the French government.

References

[1] R. Rajamani, *Vehicle Dynamics and Control*, 2nd ed. Springer, 2012.

[2] Y. Jeong and S. Yim, "Path tracking control with four-wheel independent steering, driving and braking systems for autonomous electric vehicles," *IEEE Access*, vol. 10, pp. 74 733–74 746, 2022.

[3] F. Tarhini, R. Talj, and M. Doumiati, "Adaptive look-ahead distance based on an intelligent fuzzy decision for an autonomous vehicle," *2023 IEEE Intelligent Vehicles Symposium (IV)*, 2023.

[4] L. Zhai, T. Sun, and J. Wang, "Electronic stability control based on motor driving and braking torque distribution for a four in-wheel motor drive electric vehicle," *IEEE Transactions on Vehicular Technology*, vol. 65, no. 6, pp. 4726–4739, 2016.

[5] A. M. Dizqah, B. Lenzo, A. Sorniotti, P. Gruber, S. Fallah, and J. De Smet, "A fast and parametric torque distribution strategy for four-wheel-drive energy-efficient electric vehicles," *IEEE Transactions on Industrial Electronics*, vol. 63, no. 7, pp. 4367–4376, 2016.

[6] H. Jing, F. Jia, and Z. Liu, "Multi-objective optimal control allocation for an over-actuated electric vehicle," *IEEE Access*, vol. 6, pp. 4824–4833, 2018.

[7] B. Li, H. Du, W. Li, and B. Zhang, "Integrated dynamics control and energy efficiency optimization for overactuated electric vehicles: Integrated dynamics control and energy efficiency optimisation," *Asian Journal of Control*, vol. 20, 11 2017.

[8] A. Mihály, P. Gáspár, and H. Basargan, "Maximizing autonomous in-wheel electric vehicle battery state of charge with optimal control allocation," in *2019 18th European Control Conference (ECC)*, 2019, pp. 250–255.

[9] C. Lin, S. Liang, J. Chen, and X. Gao, "A multi-objective optimal torque distribution strategy for four in-wheel-motor drive electric vehicles," *IEEE Access*, vol. 7, pp. 64 627–64 640, 2019.

[10] Z. Wang, C. Qu, L. Zhang, X. Xue, and J. Wu, "Optimal component sizing of a four-wheel independently-actuated electric vehicle with a real-time torque distribution strategy," *IEEE Access*, vol. 6, pp. 49 523–49 536, 2018.

[11] J. Torinsson, M. Jonasson, D. Yang, and B. Jacobson, "Energy reduction by power loss minimisation through wheel torque allocation in electric vehicles: a simulation-based approach," *Vehicle System Dynamics*, vol. 60, no. 5, pp. 1488–1511, 2022.

[12] A. K. Madhusudhanan and M. Corno, "Effect of a nu vinci type cvt based energy efficient cruise control on an electric vehicle's energy consumption," in *2022 European Control Conference (ECC)*, 2022, pp. 1722–1727.

[13] J. V. Alcantar and F. Assadian, "Vehicle dynamics control of an electric-all-wheel-drive hybrid electric vehicle using tyre force optimisation and allocation," *Vehicle System Dynamics*, vol. 57, no. 12, pp. 1897–1923, 2019.

[14] X. Zhang and D. Göhlich, "Integrated traction control strategy for distributed drive electric vehicles with improvement of economy and longitudinal driving stability," *Energies*, vol. 10, no. 1, 2017.

[15] F. Tarhini, R. Talj, and M. Doumiati, "Multi-objective control architecture for an autonomous in-wheel driven electric vehicle," *22nd IFAC World Congress*, 2023.

[16] W. Chen, H. Xiao, Q. Wang, L. Zhao, and M. Zhu, *Integrated vehicle dynamics and control*, 04 2016.

[17] A. Chokor, R. Talj, M. Doumiati, A. Hamdan, and A. Charara, "A comparison between a centralized multilayer lpv/h_∞ and a decentralized multilayer sliding mode control architectures for vehicle's global chassis control," *International Journal of Control*, vol. 95, pp. 1–32, 07 2020.

[18] *Protean Electric PD18 In-wheel Electric Motor Datasheet*, Protean Electric. [Online]. Available: https://www.proteanelectric.com/f/2018/05/Pd18-Datasheet-Master.pdf

[19] N. Guo, X. Zhang, Y. Zou, B. Lenzo, G. Du, and T. Zhang, "A supervisory control strategy of distributed drive electric vehicles for coordinating handling, lateral stability, and energy efficiency," *IEEE Transactions on Transportation Electrification*, vol. 7, no. 4, pp. 2488–2504, 2021.

[20] L. Guo, X. Lin, P. Ge, Y. Qiao, L. Xu, and J. Li, "Torque distribution for electric vehicle with four in-wheel motors by considering energy optimization and dynamics performance," in *2017 IEEE Intelligent Vehicles Symposium (IV)*, 2017, pp. 1619–1624.

[21] K. B. Singh, M. A. Arat, and S. Taheri, "Literature review and fundamental approaches for vehicle and tire state estimation," *Vehicle System Dynamics*, vol. 57, no. 11, pp. 1643–1665, 2019.

[22] F. E. Curtis, T. Mitchell, and M. L. Overton, "A bfgs-sqp method for nonsmooth, nonconvex, constrained optimization and its evaluation using relative minimization profiles," *Optimization Methods and Software*, vol. 32, no. 1, pp. 148–181, 2017.

[23] J. Nocedal and S. J. Wright, *Numerical Optimization*, 2nd ed. New York, NY, USA: Springer, 2006.

[24] H. Laghmara, M. Doumiati, R. Talj, and A. Charara, "Yaw moment lyapunov based control for in-wheel-motor-drive electric vehicle," *IFAC-PapersOnLine*, vol. 50, no. 1, pp. 13 828–13 833, 2017.